Cement & Concrete Composites 32 (2010) 157–163

Contents lists available at ScienceDirect

Cement & Concrete Composites

journal homepage: www.elsevier.com/locate/cemconcomp

Alkali-activated aluminosilicate composite with heat-resistant lightweight aggregates exposed to high temperatures: Mechanical and water transport properties

Lucie Zuda [a], Jaroslava Drchalová [b], Pavel Rovnaník [c], Patrik Bayer [c], Zbyněk Keršner [d], Robert Černý [a,*]

[a] Department of Materials Engineering and Chemistry, Faculty of Civil Engineering, Czech Technical University, Thákurova 7, 166 29 Prague 6, Czech Republic
[b] Department of Physics, Faculty of Civil Engineering, Czech Technical University, Thákurova 7, 166 29 Prague 6, Czech Republic
[c] Institute of Chemistry, Faculty of Civil Engineering, Brno University of Technology, Žižkova 17, 60200 Brno, Czech Republic
[d] Institute of Structural Mechanics, Faculty of Civil Engineering, Brno University of Technology, Veveří 95, 60200 Brno, Czech Republic

ARTICLE INFO

Article history:
Received 19 May 2009
Received in revised form 16 November 2009
Accepted 17 November 2009
Available online 22 November 2009

Keywords:
Alkali-activated aluminosilicate composites
Vermiculite
Mechanical properties
Water transport properties
Thermal load

ABSTRACT

A lightweight composite material with alkali-activated aluminosilicate binder is investigated. The intended use of this material is the high-temperature applications, such as the fire-protecting layers for Portland-cement based structures. Therefore, a heat-resistant mixture of expanded vermiculite and electrical porcelain is used as aggregates. Basic physical characteristics, mechanical properties and water- and water vapor transport properties are studied as functions of previous heat treatment up to 1200 °C. Experimental results show that the studied material has very good high-temperature properties which are quite superior to Portland-cement concrete. The open porosity increases only up to 7% between room temperature and 1000 °C. The material keeps 35% of its original compressive strength and 66% of its flexural strength even in the worst case of 800 °C pre-heating. After pre-heating to 1200 °C the compressive strength is found 30% higher and flexural strength three-and-half times higher than in the reference state. Liquid moisture diffusivity is after the heat treatment up to three orders of magnitude higher than in reference room-temperature conditions. The water vapor transport parameters allow fast removal of water vapor and other gaseous compounds over the whole studied heat-treatment range.

1. Introduction

Alkali-activated binders were possibly used already in ancient Mesopotamia, Egypt and Rome (see, e.g. [1,2]) but in the modern era their development began in 1940s, with the pioneering work of Purdon [3]. Since that time they became subject of numerous investigations (see, e.g. the reviews in [1,4,5]) which continue until the present.

During the last couple of decades the worldwide interest in alkali-activated binders increased remarkably for both economical and environmental reasons as alkali activation was confirmed to be applicable to waste materials, such as fly-ash or slag. Another motivation for their extended analysis was the good potential of alkali-activated aluminosilicates (AAA) for high-temperature applications. The reduced content of portlandite, which is responsible for the damage of Portland-cement based composites at 460–480 °C, in AAA was the main argument in that respect. Nevertheless, the frequency of their investigation was lower than of common cement-based composites, and the current knowledge of this type of materials remained less advanced as yet.

The basic room-temperature properties of AAA in the form of pastes, mortars and concretes resulting from slag or fly-ash activation were studied in a relatively high number of papers (e.g. [6–15]). As for the high-temperature properties, Zuda et al. [16,17] reported very good high-temperature resistance of alkali-activated slag mortar with quartz and electrical-porcelain aggregates. Fernandez-Jimenez et al. [18] found that alkali-activated fly-ash composite performed significantly better at high temperatures than the Portland cement control. Guerrieri et al. [19], on the other hand, observed thermal spalling of alkali-activated slag concrete with basalt aggregates.

The type of aggregates played a very important role also in residual mechanical properties of AAA after high-temperature exposure. While for the alkali-activated slag concrete with basalt coarse aggregates studied in [20] the reduction in compressive strength between room temperature and 800 °C was approximately 90%, for the material with quartz sand aggregates in [16] it was 80% and for that with electrical-porcelain aggregates in [17] only 70%. In the temperature range of 800–1200 °C the role of the type of aggregates was even more notable. The alkali-acti-

* Corresponding author. Tel.: +420 224354429; fax: +420 224354446.
E-mail address: cernyr@fsv.cvut.cz (R. Černý).

0958-9465/$ - see front matter © 2009 Elsevier Ltd. All rights reserved.
doi:10.1016/j.cemconcomp.2009.11.009

vated slag concrete from [20] lost at 1200 °C its strength completely but quartz and electrical-porcelain aggregates in [16,17] and provided the necessary compounds for ceramic bond formation which caused the compressive strength to increase between 800 °C and 1200 °C more than five times. As it was shown in [21], the thermal expansion properties of different aggregates were another important factor for the mechanical performance of AAA. Contrary to the results obtained for geopolymers [22,23] and alkali-activated slag pastes [20], no thermal shrinkage was observed up to 1000 °C; the thermal expansion mismatch between the contracting aluminosilicate gel and expanding aggregates resulted for the aluminosilicate composites with both quartz sand and electrical-porcelain aggregates in positive values of the apparent linear thermal expansion coefficient.

In this paper, we are coming up with an idea of lightweight composite material with alkali-activated aluminosilicate binder. The intended use of this material is the high-temperature applications, for instance fire-protecting layers for Portland-cement based structures. Therefore, a heat-resistant mixture of expanded vermiculite and electrical porcelain is used as aggregates. Expanded vermiculite is chosen for its low bulk density and high-temperature stability, electrical porcelain for its low thermal expansion in a wide temperature range and good mechanical properties.

2. Materials and technology for sample preparation

Fine-ground slag of Czech origin (12.4% residue on 0.045 mm sieve and 1.9% on 0.09 mm sieve, the specific surface 392 m^2/kg) produced by Kotouč Štramberk, Ltd., CZ was used for sample preparation. It consisted of 38.6% SiO_2, 7.2% of Al_2O_3, 38.8% of CaO, 12.9% of MgO and minority compounds. As alkali activator, water–glass solution ($Na_2O{\cdot}xSiO_2{\cdot}yH_2O$) was used. It was prepared using Portil-A dried sodium silicate preparative (Cognis Iberia, s.l., Spain). Electrical porcelain (48.6% SiO_2, 45.4% Al_2O_3, 1.0% Na_2O, 2.9% K_2O and minority compounds) provided by P–D Refractories CZ, Velké Opatovice, was used as basic heat-resistant aggregate. It comprised of three fractions with grain size 0–1 mm, 1–3 mm, 3–6 mm in 1:1:1 ratio which was chosen on the basis of previous experience with the mix design in [17]. Its porosity was 0.3%, bulk density 2350 kg m^{-3}. Expanded vermiculite (35–41% SiO_2, 6–9.5% Al_2O_3, 6–9.5% Fe_2O_3, 21.5–25.5% MgO, 2–6% CaO, 0.8% Na_2O, 3–6% K_2O and minority compounds) provided by Minko, Kutná Hora, was used as lightweight heat-resistant aggregate. Its bulk density was 75–130 kg m^{-3}, sintering temperature 1260 °C, melting temperature 1315 °C. The maximum size of vermiculite grain was about 6 mm. However, large grains disintegrated during mixing with electrical porcelain, so the maximum size was actually smaller. This size fulfilled the basic recommendation that the largest dimension of aggregate should fit in the smallest dimension of the specimen five times. However, it should be mentioned there is no official standard that would explicitly give any regulation for it.

The mix was designed on the basis of the previously designed mix with electrical porcelain only [17] in such a way that a part of electrical-porcelain aggregates was replaced by the same volume of vermiculite. The volume ratio of electrical porcelain and vermiculite of 70:30 was chosen as the most appropriate for two reasons. First, it was found as a satisfactory compromise between mechanical properties and thermal insulation properties of the hardened mix. Second, if the portion of vermiculite exceeded 50 vol.%, the mixture did not set due to high content of water, which was necessary to obtain workable mix; 30 vol.% of vermiculite was still a safe solution from this point of view.

The composition of the final mixture is presented in Table 1. The technology of sample preparation was as follows. At first, the silicate preparative was mixed with water. The solution was then mixed into the homogenized slag–electrical porcelain–vermiculite mixture using a planetary mixer. The well homogenized mixture was put into molds and vibrated. The specimens were demolded after 24 h and then stored for further 27 days in pure-water bath at laboratory temperature.

After the 28-days curing period, the specimens were dried at 110 °C and after drying subjected to thermal load. Heating of the samples to the predetermined temperature was always done with the rate of 10 K/min, then the specimens remained at that temperature for the time period of 2 h and finally they were slowly cooled. The chosen pre-heating temperatures were 200 °C, 400 °C, 600 °C, 800 °C, 1000 °C and 1200 °C.

In the experimental work, the following samples were used for every pre-treatment: bulk density, open porosity and matrix density – three specimens 50 × 50 × 23 mm, flexural strength – three specimens 40 × 40 × 160 mm, compressive strength – remainders of the specimens after bending test, water absorption – three specimens 50 × 50 × 23 mm, moisture diffusivity – three specimens 20 × 40 × 300 mm, water vapor diffusion resistance factor – three cylindrical specimens, diameter 108 mm, height 20 mm.

3. Experimental methods

3.1. Basic physical characteristics

Scanning electron microscopy (SEM) was chosen for basic characterization of structural changes after thermal loading. The scanning electron microscope JEOL JSM-U3 with 10 nm resolution was used.

The bulk density, matrix density and open porosity were the analyzed basic physical properties. The water vacuum saturation method [24] was used in the measurements. Each sample was dried in a drier to remove majority of the physically bound water. After that the samples were placed into a desiccator with deaired water. During 3 h air was evacuated with vacuum pump from the desiccator. The specimen was then kept under water not less than 24 h.

Mercury intrusion porosimetry (MIP) measurements were used for determination of pore distribution in the range of 300–0.006 μm. They were performed using the porosimeter Micromeritics POREZIZER 9310 with maximum working pressure of 200 MPa.

3.2. Mechanical properties

The compressive strength and flexural strength were determined as the mechanical properties most characteristic for aluminosilicates. The flexural strength was measured by the standard three-point bending test using a 500 kN testing device. The size of the specimens was chosen in accordance to the sample dimensions common in testing cement mortars. Every specimen was

Table 1
Composition of mixture for sample preparation.

Electrical porcelain (g)			Vermiculite (g)	Slag (g)	Alkali-activation silicate admixture (g)	Water (ml)
0–1 mm fraction	1–3 mm fraction	3–6 mm fraction				
315	315	315	44	450	90	235

positioned in such a way that the sides which were horizontal during the preparation were in the vertical position during the test. The compressive strength was determined by a compression test using the same device. It was done on the parts of the specimens broken at the bending test. The specimens were placed between the two plates of the testing device in such a way that their lateral sides adjoining during the preparation to the vertical sides of the molds were in contact with the plates. In this way, the imprecision of the geometry on the upper cut off side was not affecting negatively the experiment.

3.3. Water-vapor and water transport properties

The wet-cup and dry-cup methods were employed in the measurements of water vapor transport parameters. The specimens were water- and vapor-proof insulated by epoxy resin on all lateral sides, put into the cup and sealed by technical plasticine. The impermeability of the plasticine sealing was achieved by heating it first for better workability and subsequent cooling that resulted in its hardening. In the wet-cup method the sealed cup containing saturated K_2SO_4 solution (the equilibrium relative humidity above the solution was 97.8%) was placed into an air-conditioned room with 30% relative humidity and weighed periodically. The measurements were done at 25 ± 1 °C in a period of 4 weeks. The steady state values of mass loss determined by linear regression for the last five readings were used for the determination of water vapor diffusion coefficient. In the dry-cup method the sealed cup containing dried $CaCl_2$ (the equilibrium relative humidity above the desiccant was 5%) was placed in an air-conditioned room with 30% relative humidity. Otherwise, the measurement was done in the same way as in the wet-cup method. The water vapor diffusion resistance factor (the ratio of diffusion coefficients of water vapor in the air and in the porous body) was calculated from the measured data (see [24], for details).

The moisture diffusivity was determined using inverse analysis of moisture profiles measured at one-sided water penetration into a rod specimen in 1-D arrangement [25]. In the experimental determination of moisture profiles the specimen was fixed in horizontal position in order to eliminate the effect of gravity on moisture transport. The lateral sides of the specimen were water- and vapor-proof insulated using a plastic foil in order to simulate 1-D water transport. A viscous sponge arranging for a good contact of the specimen surface with water was put into a Perspex water-filling chamber and applied to one face side of the specimen. The sponge sucked water from a free surface being about 10 mm below the lower side of the specimen. Water in the chamber was maintained on constant level using a float. In this way, a continuous water supply to the measured specimen was achieved. After specified time of water uptake, the experiment was interrupted, the specimen cut into 1 cm thick pieces and the moisture profile determined by the gravimetric method. The experimental moisture profiles were approximated by the linear filtration method with Gaussian weights, and the moisture diffusivity calculated in dependence on moisture content using the Matano method [26].

For a comparison, the apparent value of moisture diffusivity was also determined using a simple water sorptivity experiment [25]. The specimen was water- and vapor-proof insulated on four lateral sides and the face side was immersed 1–2 mm in the water. Constant water level in the tank was achieved by a Mariotte bottle with two capillary tubes. One of them, inside diameter 2 mm, was ducked under the water level. The second one, inside diameter 5 mm, was above water level. The automatic balance allowed recording the increase of mass. The water absorption coefficient A [kg m^{-2} s$^{-1/2}$] was calculated from the sorptivity plot and used for the determination of apparent moisture diffusivity by a procedure described in [27].

4. Experimental results and discussion

4.1. Basic physical characteristics

The SEM image of the analyzed AAA composite at room temperature (Fig. 1) shows the lamellar structure of expanded vermiculite which had pores bigger than 1 μm in diameter. The contacts between the matrix and vermiculite were highly compact which was, apparently, caused by embedding the AAA matrix into the surface pores of vermiculite. Fig. 2 revealed a significant decomposition of the AAA matrix around the stable vermiculite aggregates after exposure to 1000 °C. At 1200 °C the vermiculite structure collapsed due to a beginning of sintering (Fig. 3), and large pores of about 100 μm in diameter appeared. The digital camera pictures presented in Figs. 4 and 5 (the same resolution was used in both pictures) illustrate the structural changes of the studied AAA composite between 1000 °C and 1200 °C in macro-scale. While after heating to 1000 °C (Fig. 4) no apparent changes of the surface could be observed, at 1200 °C (Fig. 5) numerous cracks visible to the naked eye emerged.

The bulk density of the studied AAA composite decreased very slowly up to 1000 °C, the open porosity measured by water vacuum saturation method similarly slowly increased (up to 7%), the matrix density remained virtually unchanged (Table 2). On the other hand, the porosity of the gel (as indicated by MIP results) increased faster with increasing pre-heating temperature than that of the whole composite. The total intrusion volume was after heating to 1000 °C more than two times higher than in the reference state. These findings confirm the desired good thermal stability of both types of aggregates up to 1000 °C. However, between 1000 °C and 1200 °C a sudden change in all basic physical characteristics appeared. The open porosity decreased by 35% as compared with 1000 °C pre-heating, the bulk density increased by about 10%, the total intrusion volume measured by MIP was more than five times lower than for the 1000 °C pre-heating and more than two times lower than in the reference state. These results

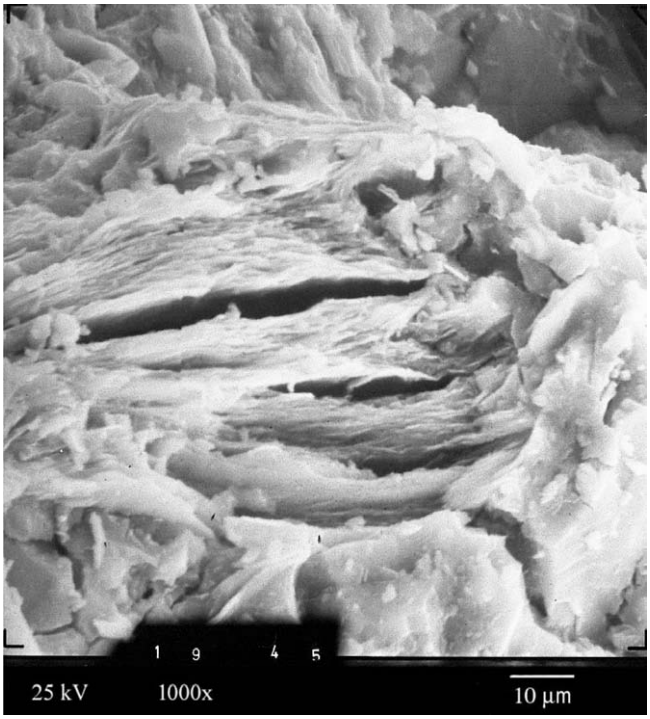

Fig. 1. SEM image of AAA composite at room temperature.

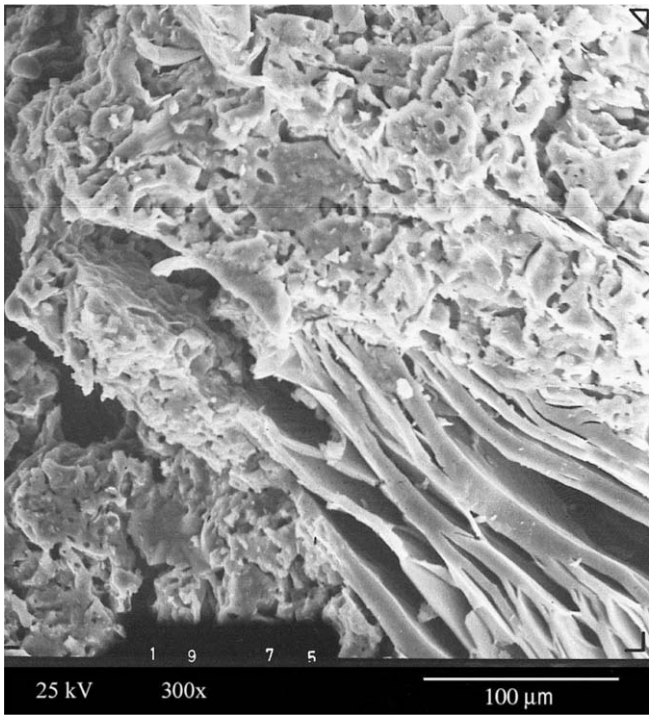

Fig. 2. SEM image of AAA composite exposed to 1000 °C.

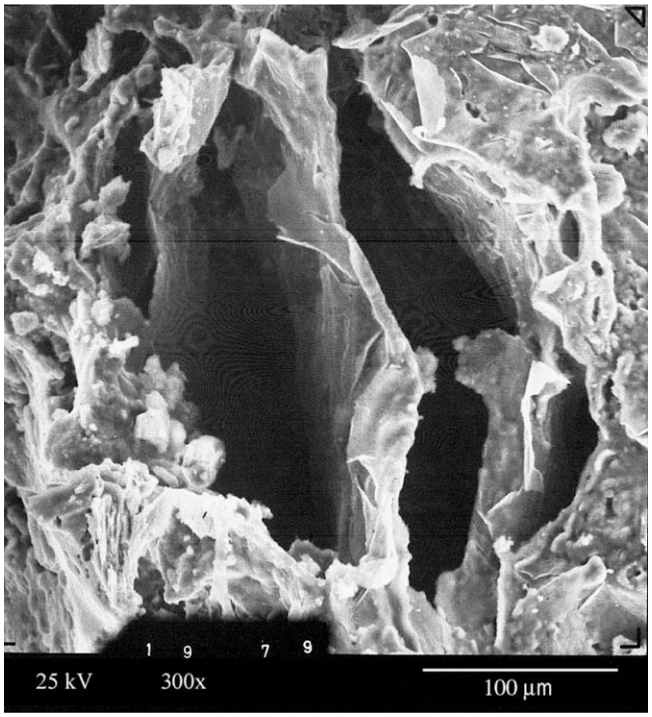

Fig. 3. SEM image of AAA composite exposed to 1200 °C.

can be explained by the structural modifications observed by SEM in Figs. 1–3.

The basic physical characteristics were compared with the AAA mix with only electrical-porcelain aggregates [17] which was designed in a similar way except for using vermiculite (electrical porcelain – each of the 0–1 mm, 1–3 mm, 3–6 mm fractions 450 g, slag – 450 g, alkali activator Portil-A – 90 g, water – 190 ml). The open

Fig. 4. Digital camera picture of specimen surface exposed to 1000 °C.

Fig. 5. Digital camera picture of specimen surface exposed to 1200 °C.

porosity of the composite material studied in this paper increased much slower with the increasing pre-heating temperature up to 1000 °C (for the composite in [17] an almost 40% increase between the reference state and 1000 °C was observed), which may indicate its better high-temperature stability. After the exposure to 1200 °C, the differences in basic physical characteristics (as compared with the composite from [17]) were within the error range of the measuring method, apparently due to the collapse of the vermiculite structure documented in Fig. 3.

The pore-distribution measurements showed that the studied AAA had already at room temperature a substantial amount of capillary pores between 1 µm and 25 µm (Fig. 6). This was probably related to the natural porosity of vermiculite. After exposure to 600 °C the volume of pores at about 3 µm in diameter increased due to dehydration of the matrix. Between 800 °C and 1000 °C the matrix was further decomposed, and while the peak at 3 µm was at first reduced almost to the room-temperature value and then re-appeared at 1000 °C, a new peak at 25 µm could be observed at both 800 °C and 1000 °C. After the exposure to 1200 °C, the capillary pores between 1 µm and 25 µm disappeared but new pores of 60 µm (and possibly higher) diameter were formed. This is in a good agreement with both SEM results (Figs. 1–3) and the visual observations (Figs. 4 and 5).

Table 2
Basic physical properties.

Heat treatment (°C)	Bulk density (kg m^{-3})	Matrix density (kg m^{-3})	Open porosity (m^3/m^3)	Total intrusion volume – MIP (cm^3/g)
25	1918	2749	0.30	0.107
200	1944	2787	0.30	0.112
400	1946	2754	0.29	0.151
600	1878	2752	0.30	0.155
800	1857	2713	0.32	0.120
1000	1856	2728	0.32	0.265
1200	2102	2635	0.20	0.045

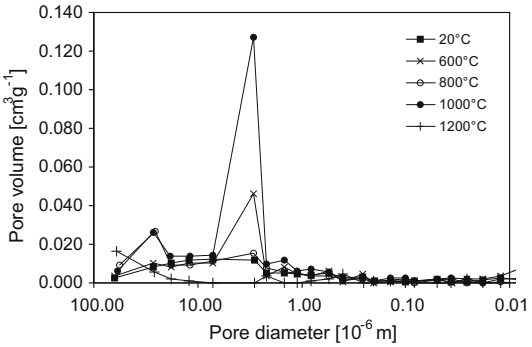

Fig. 6. Pore distribution.

4.2. Mechanical properties

The compressive strength of the AAA composite progressively decreased up to 800 °C (Table 3), which was caused at first (from 100 to 600 °C) by dehydration of the matrix, and above 600 °C by further decomposition of the dehydrated aluminosilicates. From 800 °C the compressive strength began to increase which could be explained by the formation and growth of the new crystalline phase, akermanite (see [16], for a detailed analysis). After heating to 1200 °C the surface of electrical-porcelain aggregates started to melt in the alkali environment (similarly as in the composite studied in [17]), which initiated the reaction of electrical porcelain with the partially decomposed AAA matrix. As a result, a ceramic bond was formed, which further increased the compressive strength. On the other hand, vermiculite became unstable above 1150 °C and started to sinter. Therefore, the increase of compressive strength of the investigated AAA composite was after 1200 °C pre-heating less remarkable than for that with only electrical-porcelain aggregates (the compressive strength of the composite in [17] increased two times as compared to the reference state; it was five times higher than for 1000 °C pre-heating) although the values of open porosity were similar. In a summary, the compressive strength of the lightweight AAA composite studied in this paper was expectantly lower as compared with the higher-density material in [17] but the changes due to the high-temperature treatment were moderated, apparently by the presence of vermiculite.

Table 3
Mechanical properties.

Heat treatment (°C)	Flexural strength (MPa)	Compressive strength (MPa)
25	3.3	22.6
200	2.9	21.2
400	2.7	18.4
600	2.4	14.2
800	2.2	7.9
1000	2.5	10.1
1200	11.6	29.2

The flexural strength was affected by the increasing pre-heating temperature in a similar qualitative way as the compressive strength (Table 3). The minimum was achieved for 800 °C, the maximum for 1200 °C. However, the increase of flexural strength after exposure to 1200 °C was even more considerable than of compressive strength; it was three-and-half times higher as compared to the room-temperature value.

It should be noted that for the concrete-like materials, strength data are affected by the specimen size. Due to heating, the mechanical properties change and, as a consequence, the specimens can be considered to be made with an altered material which is different from the mechanical point of view. Evaluating properties of thermally damaged specimens of equal size, without an identification of fracture process zone as it was done in this paper, provides only an approximate assessment of the true mechanical properties of the damaged material.

4.3. Water-vapor and water transport properties

The water vapor diffusion resistance factor of the analyzed AAA in both wet-cup and dry-cup arrangements was affected by the heat treatment only very little up to 600 °C (Table 4). At 800 °C and 1000 °C it decreased by approximately one-third, but after heating to 1200 °C it increased about two times and achieved higher values than at room temperature. These results are in a good qualitative agreement with the open porosity measured by water vacuum saturation method (Table 2). For the materials with a majority of capillary pores such as AAA studied in this paper the total volume of the pores is the most important factor affecting water vapor transport because viscous water vapor flow occurs in the most of the pores (for a detailed analysis, see [25]).

The measured values of water vapor diffusion resistance factor (Table 4) were typically 30–40% lower than those of the AAA with only electrical porcelain in [17]. This is an advantageous feature for a material which can potentially be utilized as fire-protecting layer. The high water vapor transport capability enables fast removal of water vapor and other gaseous compounds, thus reduces the risk of damage induced by high gas pressure in the pore system.

Fig. 7 shows that the moisture diffusivity κ depended on moisture content in a very significant way. The differences in κ corresponding to the lowest and highest moisture values were almost two orders of magnitude. In the reference state without thermal treatment, the moisture diffusivity values were relatively high already, about one order of magnitude higher than for ceramic brick, for instance. This reflected the significant amount of capillary pores in the μm range in the material (Fig. 6). The increase of moisture diffusivity with increasing pre-heating temperature was up to 600 °C moderate only. However, at 800 °C and 1000 °C one to two orders of magnitude increase was observed in the whole range of moisture content. This was clearly related to the increase of volume of capillary pores >1 μm in the matrix observed in pore-distribution measurements (Fig. 6). The most significant increase in κ

Table 4
Water-vapor and water transport properties.

Heat treatment (°C)	Water vapor diffusion resistance factor (–)		Apparent moisture diffusivity (10^{-6} m^2 s^{-1})
	Dry-cup	Wet-cup	
25	17	9	0.21
200	17	9	0.28
400	17	9	0.47
600	15	10	0.62
800	10	7	15.66
1000	10	7	13.62
1200	23	14	37.50

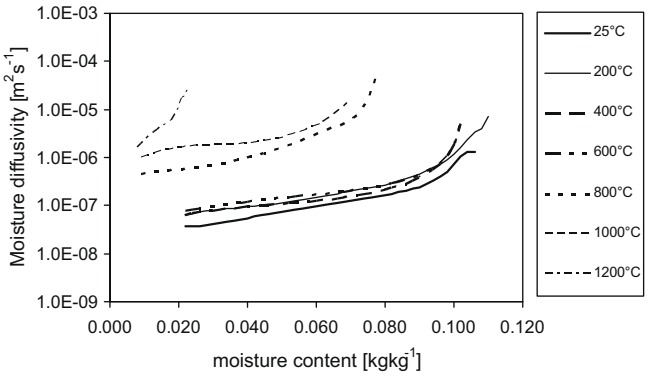

Fig. 7. Moisture diffusivity as a function of moisture content.

was found after heating to 1200 °C, about three orders of magnitude as compared to the reference room-temperature values. In this case, the appearance of wide cracks (Figs. 3 and 5) was the most important factor; the cracks acted as preferential paths for liquid water transport.

In a comparison with the AAA composite with only electrical-porcelain aggregates from [17], the increase in moisture diffusivity of the material studied in this paper was for higher pre-heating temperatures remarkably higher (for the composite studied in [17] the apparent moisture diffusivity was in the range of 3.2–3.9×10^{-7} m^2 s^{-1} for the pre-heating temperatures of 600–1200 °C). This is a positive factor for the intended high-temperature applications. High moisture diffusivity in the conditions of high temperature gradients makes possible fast removal of liquid water on the cold side which should lead to the decrease of gas pressure in the pore space.

The apparent moisture diffusivity calculated from water absorption coefficient systematically increased with the increasing pre-heating temperature (Table 4). Similarly as with the moisture-dependent moisture diffusivity, up to 600 °C the changes were relatively moderate, at 800–1200 °C the apparent moisture diffusivity was two to three orders of magnitude higher than in the reference state at room temperature. A comparison of results in Fig. 7 and Table 4 showed that the apparent moisture diffusivities corresponded with the moisture-dependent moisture diffusivities at higher moisture content. This was in a qualitative agreement with the results reported before for an extruded porcelain mixture [28].

5. Conclusions

The measurements of basic physical characteristics and mechanical and water transport properties of lightweight alkali-activated aluminosilicate composite with heat-resistant and porous aggregates after high-temperature exposure in this paper showed that it is suitable for the intended high-temperature applications, such as the fire-protecting layers for Portland-cement based structures. The main results can be summarized as follows:

- The expanded-vermiculite aggregates increased the porosity of the composite already in the room-temperature conditions which was their primary purpose. An additional benefit was the embedding of the AAA matrix into their surface pores which helped to stabilize the microstructure in the high-temperature range up to at least 1000 °C. This stabilization was reflected in a very slow increase of the open porosity of the composite with the heat-treatment temperature increase up to 1000 °C.
- The electrical-porcelain aggregates contributed to the high-temperature stability of the composite primarily by their low thermal expansion in wide temperature range and good mechanical properties. In addition, after heating to 1200 °C they started to melt in the alkali environment which initiated the reaction of electrical porcelain with the partially decomposed AAA matrix and promoted the ceramic bond formation. This led to further stabilization of the microstructure of the composite, despite the collapse of the vermiculite structure at 1150–1200 °C which led to a sudden decrease of porosity. Thus, the combination of expanded-vermiculite and electrical-porcelain aggregates could be considered as successful solution.
- The compressive strength of the AAA composite decreased with the temperature of the heat treatment up to 800 °C where it was equal to ~35% of its room-temperature value, due to the gradual thermal decomposition of the aluminosilicate matrix. However, from 800 °C the compressive strength began to increase, apparently due to the formation and growth of the new crystalline phase, akermanite. After heating to 1200 °C the value of compressive strength already was approximately 30% higher than at room temperature, despite the appearance of cracks visible by the naked eye. This was quite superior behavior, when compared to Portland-cement based composites.
- The flexural strength was affected by the increasing pre-heating temperature in a similar qualitative way as the compressive strength. The minimum was achieved after heating to 800 °C where the flexural strength decreased to ~66% of the room-temperature value, the maximum at 1200 °C where it was three-and-half times higher than at room temperature. Once again, rather incomparable results with Portland-cement concrete.
- The water vapor diffusion resistance factor μ of the analyzed AAA composite remained up to 600 °C almost unaffected by the heat treatment. At 800 °C and 1000 °C it decreased by approximately one-third, but after heating to 1200 °C it increased about two times and achieved higher values than at room temperature. The μ values were sufficiently low to allow fast removal of water vapor and other gaseous compounds. Thus, the risk of damage induced by the possibly increased gas pressure in the pore system was on an acceptable level.
- The liquid moisture diffusivity was relatively high already at room temperature, about one order of magnitude higher than for ceramic brick. Its increase with increasing pre-heating temperature was up to 600 °C moderate only. For higher temperatures, an up to three orders of magnitude increase was observed in the whole range of moisture content. This was related to the increase of volume of capillary pores, and at 1200 °C also by the appearance of wide cracks which acted as preferential paths for liquid water transport. The high moisture diffusivity in the conditions of high temperature gradients is a positive factor for the intended high-temperature applications because it makes possible fast removal of liquid water on the cold side which should lead to the decrease of gas pressure in the pore space.
- In a comparison with higher-density aluminosilicate composite with only electrical-porcelain aggregates studied in [17], the lightweight composite analyzed in this paper had lower strength but the changes due to the high-temperature treatment were moderated, apparently by the presence of vermiculite. The liquid water and water vapor transport properties were higher than of the composite in [17] which is advantageous for a material that can potentially be utilized as a fire-protecting layer.
- It should be mentioned that compatibility of the protective layer and substrate is an important issue for fire-protecting materials which was, however, not addressed in this paper. Therefore, before the final use of the designed composite as a fire-protecting layer in specific applications in building practice testing of the protective layer–substrate system might be necessary.

Acknowledgements

This research was supported by the Ministry of Education, Youth and Sports of Czech Republic, under Project No. MSM: 6840770031.

References

[1] Roy DM. Alkali-activated cements. Opportunities and challenges. Cem Concr Res 1999;29:249–54.
[2] Glukhovsky VD. Soil silicates. Kiev: Gosstroi Publishers; 1959.
[3] Purdon AO. The action of alkalis on blast furnace slag. J Soc Chem Ind 1940;59:191–202.
[4] Pacheco-Torgal F, Castro-Gomes J, Jalali S. Alkali-activated binders: a review. Part 1. Historical background, terminology, reaction mechanisms and hydration products. Constr Build Mater 2008;22:1305–14.
[5] Pacheco-Torgal F, Castro-Gomes J, Jalali S. Alkali-activated binders: a review. Part 2. About materials and binders manufacture. Constr Build Mater 2008;22:1315–22.
[6] Palomo A, Grutzeck MW, Blanco MT. Alkali-activated fly ashes. A cement for the future. Cem Concr Res 1999;29:1323–9.
[7] McCarter WJ, Chrisp TM, Starrs G. The early hydration of alkali-activated slag: developments in monitoring techniques. Cem Concr Compos 1999;21:277–83.
[8] Puertas F, Fernandez-Jimenez A. Mineralogical and microstructural characterisation of alkali-activated fly ash/slag pastes. Cem Concr Compos 2003;25:287–92.
[9] Douglas E, Bilodeau A, Malhotra VM. Properties and durability of alkali-activated slag concrete. ACI Mater J 1992;89:509–16.
[10] Collins FG, Sanjayan JG. Workability and mechanical properties of alkali activated slag concrete. Cem Concr Res 1999;29:455–8.
[11] Bakharev T, Sanjayan JG, Cheng YB. Effect of admixtures on properties of alkali activated slag concrete. Cem Concr Res 2000;30:1367–74.
[12] Collins F, Sanjayan J. Unsaturated capillary flow within alkali activated slag concrete. J Mat Civil Eng 2008;20:565–70.
[13] Yang KH, Song JK, Ashour AF, Lee ET. Properties of cementless mortars activated by sodium silicate. Constr Build Mater 2008;22:1981–9.
[14] Al-Otaibi S. Durability of concrete incorporating GGBS activated by water–glass. Constr Build Mater 2008;22:2059–67.
[15] Yang KH, Song JK. Workability loss and compressive strength development of cementless mortars activated by combination of sodium silicate and sodium hydroxide. J Mat Civil Eng 2009;21:119–27.
[16] Zuda L, Pavlík Z, Rovnaníková P, Bayer P, Černý R. Properties of alkali activated aluminosilicate material after thermal load. Int J Thermophys 2006;27:1250–63.
[17] Zuda L, Bayer P, Rovnaník P, Černý R. Mechanical and hydric properties of alkali-activated aluminosilicate composite with electrical porcelain aggregates. Cem Concr Compos 2008;30:266–73.
[18] Fernandez-Jimenez A, Palomo A, Pastor JY, Martin A. New cementitious materials based on alkali-activated fly ash: performance at high temperatures. J Am Ceram Soc 2008;91:3308–14.
[19] Guerrieri M, Sanjayan J, Collins F. Effect of slag on the performance of concretes in hydrocarbon fire. ACI SP-255: designing concrete structures for fire safety. Farmington Hills (MI): American Concrete Institute; 2008. p. 23–45.
[20] Guerrieri M, Sanjayan JG, Collins FG. Residual compressive behavior of alkali activated concrete exposed to elevated temperatures. Fire Mater 2009;33:51–62.
[21] Zuda L, Černý R. Measurement of linear thermal expansion coefficient of alkali-activated aluminosilicate composites up to 1000 °C. Cem Concr Compos 2009;31:263–7.
[22] Duxson P, Lukey GC, van Deventer JSJ. Thermal evolution of metakaolin geopolymers. Part 1. Physical evolution. J Non-Cryst Solids 2006;352:5541–55.
[23] Duxson P, Lukey GC, van Deventer JSJ. Physical evolution of Na-geopolymer derived from metakaolin up to 1000 °C. J Mater Sci 2007;42:3044–54.
[24] Roels S, Carmeliet J, Hens H, Adan O, Brocken H, Černý R, et al. Interlaboratory comparison of hygric properties of porous building materials. J Therm Envelop Build Sci 2004;27:307–25.
[25] Černý R, Rovnaníková P. Transport processes in concrete. London: Spon Press; 2002.
[26] Matano C. On the relation between the diffusion coefficient and concentration of solid metals. Jpn J Phys 1933;8:109–13.
[27] Kumaran MK. Moisture diffusivity of building materials from water absorption measurements. J Therm Envelop Build Sci 1999;22:349–55.
[28] Drchalová J, Černý R. A simple gravimetric method for determining the moisture diffusivity of building materials. Constr Build Mater 2003;17:223–8.